KfK 5011
April 1992

Corrosion Studies on Selected Packaging Materials for Disposal of Heat-Generating Radioactive Wastes in Rock-Salt Formations

E. Smailos, W. Schwarzkopf, J. A. Gago, I. Azkarate
Institut für Nukleare Entsorgungstechnik

Kernforschungszentrum Karlsruhe

Kernforschungszentrum Karlsruhe
Institut für Nukleare Entsorgungstechnik

KfK 5011

CORROSION STUDIES ON SELECTED PACKAGING MATERIALS FOR DISPOSAL OF HEAT-GENERATING RADIOACTIVE WASTES IN ROCK-SALT FORMATIONS

E.Smailos, W. Schwarzkopf, J.A. Gago *, I. Azkarate **

* ENRESA, Spain
** INASMET, Spain

Work performed within the framework of the 1991-1994 programme of the European Atomic Energy Community: "Management and storage of radioactive waste". Task 3: Characterization and qualification of waste forms, packages and their environment. EC-Research Contract No. FI2W-CT90-0030.

Kernforschungszentrum Karlsruhe GmbH, Karlsruhe

Kernforschungszentrum Karlsruhe GmbH
Postfach 3640, 7500 Karlsruhe 1

ISSN 0303-4003

Summary

In previous corrosion studies, carbon steels and the alloy Ti 99.8-Pd were identified as promising materials for heat-generating nuclear waste packagings that could act as a barrier in a rock-salt repository. To characterize the corrosion behaviour of these materials in more detail, a research programme including laboratory-scale and in-situ corrosion studies has been undertaken jointly by KfK and ENRESA/INASMET. Besides carbon steels and Ti 99.8-Pd, also Hastelloy C4 and some Fe-base materials are being examined in order to complete the results available to date.

In the period under review, long-term immersion tests of up to one year and stress corrosion cracking studies (slow strain rate tests) were perfomed on three preselected carbon steels (one unalloyed, two low-alloyed steels) in disposal relevant brines ($MgCl_2$-rich and NaCl-rich) at 150°C-170°C. Moreover, in-situ corrosion experiments were conducted on electron-beam welded cast-steel tubes plated with either Ti 99.8-Pd or Hastelloy C4 in brines with a view to examine the influence of selected container manufacturing characteristics on the corrosion of these materials.

The results of the immersion tests on the low-alloyed steels TStE 460 and 15Mn Ni6.3 at 150°C have shown that both steels are subjected to general corrosion in all test brines. In the $MgCl_2$-rich brines, clearly higher corrosion rates (90-175µm/a) were obtained for the steels than in the NaCl-rich brine (29-72µm/a). Such values imply corrosion allowances technically acceptable for a thick-walled packaging. Pitting did not occur on the parent materials. The same is true also for the submerged arc welded (SAW) steel specimens tested in the NaCl-rich brine. In the $MgCl_2$-rich brines, however, severe local corrosion attacks were detected for both steels in the heat-affected zone of the welded specimens. In the slow strain rates tests (10^{-4} - 10^{-6} s^{-1}) at 170°C in an $MgCl_2$-rich brine, no indication of stress corrosion cracking was found for the hot-rolled steels TStE 460 and fine-grained steel TStE 355 (unalloyed steel). On the contrary, a clear susceptibility to stress corrosion cracking was observed for the forged steel 15Mn Ni6.3.

In the cast-steel tube with a corrosion protection of Ti 99.8-Pd, no indication of corrosion was observed on the electron-beam welds or on the explosion plated material neither in $MgCl_2$-rich brine nor in NaCl brine. The cast-steel tube with a corrosion protection layer of Hastelloy C4 also was found to be resistant to any kind of corrosion in the NaCl-brine. In the $MgCl_2$-rich brine, however, small pitting (15µm) was observed after 1.5 years on the passive surface layer that was formed. Further laboratory-scale and in-situ corrosion studies are in progress.

Korrosionsuntersuchungen an ausgewählten Verpackungsmaterialien für die Endlagerung von wärmeerzeugenden radioaktiven Abfällen in Steinsalzformationen

Zusammenfassung

Bisherige Korrosionsuntersuchungen ergaben, daß Kohlenstoffstähle und die Legierung Ti 99.8-Pd aussichtsreiche Materialien für langzeitbeständige Verpackungen zur Endlagerung von wärmeerzeugenden Abfällen in Steinsalzformationen sind. Zur detaillierten Charakterisierung des Korrosionsverhaltens dieser Werkstoffe werden von KfK und ENRESA/INASMET in einem gemeinsamen Forschungsprogramm weitergehende Untersuchungen durchgeführt. Neben Stählen und Ti 99.8-Pd werden zur Vervollständigung der bisher vorliegenden Ergebnisse auch Hastelloy C4 und einige Eisenbasiswerkstoffe untersucht.

Im Berichtszeitraum wurden Langzeit-Immersionsversuche bis zu einem Jahr und Spannungsrißkorrosionsexperimente bei langsamen Dehnungsraten an drei ausgewählten Stählen (ein unlegierter und zwei niedriglegierte Stähle) in endlagerrelevanten Salzlösungen ($MgCl_2$- und NaCl-reich) bei 150°C - 170°C durchgeführt. Darüber hinaus wurden in situ-Korrosionsexperimente an elektronenstrahlgeschweißten und mit Ti 99.8-Pd bzw. Hastelloy C4 platierten Rohrabschnitten aus Stahlguß in Salzlösungen durchgeführt. Ziel war es, den Einfluß ausgewählter Herstellungsbedingungen für Behälter auf die Korrosion dieser Werkstoffe zu prüfen.

Die bisher vorliegenden Ergebnisse aus den Immersionsversuchen bei 150°C zeigen für TStE 460 und 15MnNi 6.3 einen flächenmäßigen Korrosionsangriff in allen Prüflösungen. In den $MgCl_2$-reichen Lösungen waren die Korrosionsraten der Stähle mit 90-175µm/*a* deutlich höher als in der NaCl-reichen Lösung (29-72µm/*a*). Solche Werte führen zu technisch akzeptablen Korrosionszuschlägen für eine dickwandige Verpackung. Lochkorrosion wurde bei den Grundmaterialien nicht festgestellt. Das gleiche gilt auch für die unterpulvergeschweißten Stahlproben in der NaCl-reichen Lösung. In den $MgCl_2$-reichen Lösungen traten jedoch in der Wärmeeinflußzone der geschweißten Stahlproben starke lokale Korrosionsangriffe auf. Bei den Korrosionsuntersuchungen in einer $MgCl_2$-reichen Lösung bei 170°C und langsamen Dehnungsraten von 10^{-4} - 10^{-6} s^{-1} war keine Empfindlichkeit der warmgewalzten Stähle TStE 460 undTStE 355 (unlegierter Feinkornbaustahl) gegenüber Spannungsrißkorrosion festzustellen. Der Schmiedestahl 15MnNi 6.3 hingegen erwies sich unter diesen Bedingungen als anfällig gegenüber Spannungsrißkorrosion.

Bei den Stahlguß-Rohrabschnitten mit einem Korrosionsschutz aus Ti 99.8-Pd war sowohl in der $MgCl_2$-reichen als auch in der NaCl-Lösung weder an den Schweißnähten noch am Korrosionsschutzmaterial ein Korrosionsangriff festzustellen. Das gleiche gilt auch für die Stahlguß-Rohrabschnitte mit einem Korrosionsschutz aus Hastelloy C4 in der NaCl-Lösung. In der $MgCl_2$-reichen Lösung jedoch trat bei Hastelloy C4 Lochkorrosion auf, wobei allerdings die Angriffstiefe nach 1.5 Jahren nur 15µm betrug. Weitere Labor- und in-situ Korrosionsuntersuchungen sind im Gange.

Contents

1. Introduction and objectives

Disposal of radioactive wastes in deep rock-salt formations is based on the concept of isolating the radionuclides from the biosphere by a combination of geological and engineered barriers. One element of this multi-barrier concept in the disposal of heat-generating wastes (vitrified HLW, spent fuel) is the waste packaging. Accordingly, studies have been undertaken by KfK within the framework of the previous EC research programme to develop long-term resistant packagings that could act as a barrier during the elevated-temperature phase in the disposal area which lasts a few hundred years. For this purpose, packaging materials must be determined that meet the requirement of long-term corrosion resistance in rock salt and in salt brines, which may be present in the disposal area under certain conditions.

In previous corrosion studies [e.g. 1,2] carbon steels and the titanium alloy Ti 99.8-Pd were identified as the most promising materials for the manufacturing of long-lived packagings in rock salt. To characterize the corrosion behaviour of these materials in more detail, a 1991-1994 EC research programme is being performed jointly by KfK and ENRESA/INASMET.

The research programme consists of two parts. The KfK part is aimed at studying the influence of important parameters on the corrosion behaviour of preselected carbon steels and Ti 99.8-Pd in disposal relevant salt brines. These parameters are: temperature, gamma radiation and selected characteristics of packaging manufacturing. Both laboratory-scale and in-situ corrosion studies in the Asse salt mine are being carried out. Besides carbon steels and Ti 99.8-Pd, also Hastelloy C4 and the Fe-base materials nodular cast iron, Ni-Resist D2 and Ni-Resist D4 are being examined in the in-situ corrosion experiments in order to complete the results available to date.

The second part of the corrosion studies concerns in the investigation of the resistance of carbon steels to stress corrosion cracking in a disposal relevant salt brine at various strain rates and temperatures by ENRESA/INASMET. For this purpose, the slow strain rate technique (SSRT) is being applied. These studies serve to complete the results available so far on statically loaded U-bend specimens. In addition to the corrosion experiments, a statistical analysis of the corrosion data will

be performed with a view to determine the probability of container failure. The entire research programme is coordinated by KfK.

In the present paper, the progress achieved in the research programme until the end of 1991 shall be described.

2. Long-term laboratory-scale corrosion studies on low-alloyed steels (KfK)

In the Federal Republic of Germany, low-alloyed steels such as 15 MnNi6.3 and TStE 460 are discussed as container materials for the disposal of spent fuel in the galleries of a rock-salt repository. To examine the long-term corrosion behaviour of these steels in brine environments relevant for a repository, immersion experiments lasting of up to 18 months are being performed at 150°C in three salt brines. In the period under review, the experiments of up to 12 months have been completed and the results are reported.

2.1 Experimental

The TSt E 460 steel was examined in the hot-rolled and annealed condition, the 15 MnNi 6.3 steel in the forged and annealed condition.

The steels had the following compositions (wt.%):

TSt E 460:	0.18 C; 0.34 Si; 1.5 Mn; 0.51 Ni; 0.15 V; bal. Fe
15 MnNi6.3:	0.17 C; 0.22 Si; 1.59 Mn; 0.79 Ni; bal. Fe

Three salt brines differing qualitatively and quantitatively were used as corrosion media. Two of them (brines 1 and 2) are highly concentrated in $MgCl_2$, the third (brine 3) has a high concentration of NaCl. The compositions, pH-values and O_2 - contents of the brines are given in Table I. The pH-values given are relative data and were measured using a glass electrode. The O_2 - values were determined by a polarographic method using an O_2 - sensor; reference were the saturation values (1.0 - 1.4 mg O_2 /l) obtained by the Winkler method.

Besides specimens of the parent materials also submerged-arc welded (SAW) specimens in the forged and annealed condition were investigated in order to examine the influence of this welding technique selected for the spent fuel disposal

container (POLLUX) closure on the corrosion. The 15 MnNi 6.3 welded specimens were taken from a original welded lid of the POLLUX container. The TStE 460 welded specimens were prepared from a welded lid simulated by welding together two rings. Plane specimens having the dimensions of 40 mm x 20 mm x 4 mm were used.

The experiments at 150°C were performed at a brine volume to specimen surface ratio (V/S) of 5ml/cm^2, i.e. for an excess of the corrodent. In order to avoid evaporation of the brines at the high test temperature, stainless steel pressure vessels with corrosion resistant PTFE inserts were used. All experiments were carried out at an equilibrium pressure of 0.4 MPa.

2.2 Post-test examination of the specimens

When the specified test durations (4,8 and 12 months) have been achieved, the specimens were removed from the brines and treated according to the ASTM guidelines. For this, the specimens were freed from the adhering salts and corrosion products by cleaning in distilled H_2O at 60°C and pickling in the Clark solution (37% HCl + Sb_2O_3 + $SnCl_2$) with subsequent cleaning in distilled H_2O and alcohol. After drying, the specimens were examined for general and local corrosion. The general corrosion was calculated from the gravimetrically determined integral weight losses and the material density. The examination for local corrosion was made by microscopic evaluation, measurements of pit depth, surface profilometry and metallography. Additional information on the corrosion mechanism was obtained from the analysis of the corrosion products by means of X-ray diffraction (XRD).

2.3 Results

The general corrosion of the steels (parent materials) at 150°C in the three brines, expressed as the thickness reduction of the specimens, is plotted in Fig.1. In all brines, a linear increase of the values with time occurred. The linear corrosion rates of the steels in the various brines are compiled in Table II. The lowest corrosion rates occurred in the NaCl-rich brine 3 with values of 29 µm/a (TStE 460) and 72 µm/a (15 MnNi 6.3), respectively. In the $MgCl_2$-rich brines 1 (Q-brine) and 2, clearly higher corrosion rates (90-175 µm/a for TStE 460, 112-127µm/a for 15 MnNi 6.3) were obtained compared to the values of the NaCl-rich brine. This is attributed to the formation of HCl from the hydrolysis of $MgCl_2$. The acceleration of the steel

corrosion in brines containing high amounts of $MgCl_2$ is in line with the results reported by Westerman et al. [3].

It is evident from the metallographic examinations and the surface profiles that the unwelded steels (parent materials) were resistant to pitting corrosion in all three brines. A non-uniform corrosion was observed for both steels in the test brines which is attributed to inhomogeneities of the steel composition. However, the maximum penetration depth of this uneven corrosion attack corresponded to the values of the average thickness reduction. Characteristic optical micrographs of the steels TStE460 and 15MnNi6.3 after a 12-month exposure to brine 1 (Q-brine) at 150°C are shown in Fig. 2.

Welding did not influence noticeably the corrosion behaviour of the steels in the NaCl-rich brine 3. The SAW specimens underwent a non-uniform corrosion attack as did the unwelded specimens, and the general corrosion rates corresponded to the values obtained for the parent materials. In the $MgCl_2$-rich brines, however, considerable corrosion attacks were detected for both steels in the heat-affected zone (Tab.III). The depth of these corrosion attacks increased with exposure time to the brines and reached after 1 year values between 1.5 mm and 3.9 mm, depending on the steel and the brine. Fig.3 shows optical micrographs of welded specimens of the steels TStE 460 and 15 MnNi6.3 after a 12-month exposure to brine 1.

The corrosion products formed on the surface of the steel specimens were analysed by X-ray diffraction. For specimens exposed for 12 months to the NaCl-rich brine, Fe_3O_4 (magnetite) was identified. In the $MgCl_2$-rich brines, (Fe, Mg) $(OH)_2$ of the amakinite structure was found, with no evidence of Fe_3O_4.

3. In-situ corrosion studies on cast-steel tubes plated with Ti 99.8-Pd / Hastelloy C4 (KfK)

On the basis of the laboratory - scale corrosion results obtained so far and considering mechanical aspects, a thick-walled carbon steel container with or without a corrosion protection made of Ti 99.8-Pd was identified for the packaging of the HLW wastes [4,5]. As an alternative to Ti 99.8-Pd, the suitability of Hastelloy C4 as corrosion protection material is being investigated.

An important aspect of the in-situ studies is the investigation of the influence of selected container manufacturing characteristics (e.g. sealing technique, application mode of the corrosion protecting layer on the steel) on the corrosion behaviour of the materials. For this, eighteen carbon-steel tubes with and without a corrosion protection layer are being examined under simulated disposal condigions in heated boreholes in the Asse salt mine.

First results obtained for the tubes have already been reported [6]. In the period under review, the investigations on cast-steel tubes plated with either Ti 99.8-Pd or Hastelloy C4 have been continued.

3.1 Test field and details of the specimens

The configuration and dimensions of the underground test field at the 775m-level in the Asse salt mine are shown in Fig.4. The rock salt taken from the test field boreholes had the following average composition (in wt.%): Na^+: 38.3; K^+: 0.33; Ca^{2+}: 0.17; Mg^{2+}: 0.16; Cl^-: 58.02; SO_4^{2-}: 2.47; H_2O: 0.1.

In these experiments, four tubes (500 mm length, 40 mm outside diameter, 10 mm thickness) of cast steel (GS 16 Mn 5), two of them with a corrosion protection layer of Ti 99.8-Pd and two of Hastelloy C4 applied by explosion plating and EB-welding, were examined for corrosion attacks under simulated disposal conditions.

The materials used had the following compositions (in wt.%):

Cast steel:	0.16 C: 0.66 Si; 1.51 Mn; 0.02 P + S; bal. Fe.
Hastelloy C4:	15.5 Cr; 15.3 Mo; 0.8 Fe; bal. Ni.
Ti 99.8-Pd:	0.2 Pd; 0.03 Fe; bal. Ti

The materials and the design of the specimens are shown in Fig.5. The specimens consisted of nine tube sections (50 mm length, 40 mm outside diameter, 10 mm thickness) and a bottom part explosive plated with Ti 99.8-Pd or Hastelloy C4. The specimen surface was mechanically finished by means of overturning. The tube sections were joined by EB-welding with a view to simulate the container closing technique. This gave a tube of 500-mm total length. More detailed information on the manufacturing of the specimens can be found elsewhere [7].

3.2 Test conditions and experimental setup

The corrosion behaviour of the cast-steel tubes plated with either Ti 99.8-Pd or Hastelloy C4 was tested under the conditions of a hypothetical inflow of NaCl brine or Q-brine ($MgCl_2$-rich) into the HLW boreholes during the initial disposal phase, while the annular gap between the container and the borehole wall is still open. The tubes were placed into heated vertical boreholes of 2 m depth located at the 775 m level of the ASSE salt mine (see Fig. 6). The 1-mm-wide annular gap between the tube and the borehole wall was filled with 100 ml saturated NaCl brine (26.9 wt.% NaCl, 73.1 wt.% H_2O) or Q-brine (26.8 wt.% $MgCl_2$, 4.7 wt.% KCl, 1.4 wt.% $MgSO_4$, 1.4 wt.% NaCl, 65.7 wt.% H_2O). The maximum temperature of 200°C (conforming with the German disposal concept) was set at the borehole wall using a heater.

The vertical temperature profile developed during the experiment at the contact surface between the tube and the borehole wall, and the radial temperature distribution between two boreholes are shown in Fig.7. The maximum temperature of 200°C occurred in the center of the heated zone, and the minimum temperature of 90°C was measured in the upper tube zone. The temperature in the center between two boreholes nearly corresponded to the rock salt temperature of about 32°C at the 775 m level. The temperature was measured using NiCr-Ni thermocouples. In order to avoid invalidation of the corrosion results due to the corrosion induced by the contact of thermocouples and tube surface, the temperature measurements were performed in reference boreholes of identical experimental setup. The pressure in the annular gap of the actual test borehole was measured continuously with a manometer which was introduced into the brine inlet tube. The maximum pressure measured was 0.28 MPa. This corresponds to a salt brine boiling point of 140°C. This means that the water contained in the brine evaporates at points of elevated temperature and recondenses at the upper cooler end of the tubes (90°C).

The pressure and temperature at the tube surface were measured in reference boreholes using strain gauges and thermocouples. The measurements have shown that the first contact of the borehole wall with the tube due to rock pressure occurred after about six months. On the basis of the results obtained in an identical preliminary test [7], complete closure of the 1-mm-wide annular gap should haven taken place after approximately twelve months.

3.3 Post test examination of the cast-steel tubes

After a test period of eighteen months, the cast-steel tubes plated with either Ti 99.8 - Pd or Hastelloy C4 were retrieved by overcoring. The salt drilling cores obtained (1m length, 120 mm outside diameter) were cut into two half shells. A visual inspection of the tubes and the drilling cores was carried out. The loosely attached rock salt products were moved mechanically from each tube. Then, the tubes were cleaned with alcohol. After cleaning, the tubes were subjected to post test examination for corrosion attack by means of surface profilometry, scanning electron microscopy (SEM) and metallography. The effects in the surrounding rock salt (e.g. migration of brine) were investigated in different segments of the drilling cores by means of microscopic evaluation of the microsections.

3.4 Results

The visual inspection of the drilling core indicated that the 1-mm-annular gap between the tubes and the borehole wall existing at the beginning of the tests had completely closed. The damp and shining zones of the cutting surface of the drilling cores are proof that the brines added were not consumed by corrosion. Below the ceramic insulation in the cooler upper part of the tubes ($T = 90°C$), dissolved salt was clearly visible, which is attributed to the condensation of water vapour. The microscopic evaluation of microsections taken from the drilling cores revealed that the heat and the brines added caused changes in the surrounding rock salt. Zones of crystallized brine, corroded grain boundaries of rock salt etc. were observed. A publication describing the effects above in detail is in preparation.

The examination of the cast-steel tubes by means of stereo-microscopy and surface profilometry has shown that those tubes plated with Ti 99.8-Pd were resistant to corrosion in both brines. Neither on the overturning surface nor on the hot-rolled and EB-welded Ti 99.8-Pd has shown any signs of local corrosion. Even a crack produced by a steel needle to simulate severe conditions during the handling of the containers did not stimulate a corrosion attack. These results confirm the findings of previous long-term immersion tests [7] and electrochemical corrosion studies [8] which indicate that the passive oxide layer (mainly consisting of Ti O_2) formed on the surface of Ti 99.8-Pd is very stable in salt brines.

The cast-steel tube with a corrosion protection of Hastelloy C4 was resistant to local corrosion in the NaCl brine. In the $MgCl_2$-rich Q-brine, however, a large number of ruptures were detected on the Hastelloy surface layer. They preferably occurred at the overturning surface exposed to test temperatures between 150°C and 200°C. The ruptures are marked on the tube section shown in Fig.8a. The corrosion attacks on the surface of Hastelloy C4 (Fig.8b) covered a mean area of about 1 mm^2. Comparative metallographic examinations of non-etched specimens before and after 1.5 years exposure to Q-brine revealed small pits with a maximum depth of 5 µm (see Fig.8c).

Detailed investigations of the corrosion attack of Hastelloy C4 by means of scanning electron microscopy (Fig.8d) have shown

- the complete destruction of the surface layer by converging pits of 1-2 µm in size;
- the development of a new pattern of pits with approximately 10 µm in diameter and about 10-15 µm in depth.

The corrosion results obtained for Hastelloy C4 in Q-brine are in good agreement with those of previous electrochemical and long-term corrosion studies [9, 10] which have shown that this material is susceptible to local corrosion in this brine at elevated temperature. The higher corrosivity of the Q-brine compared to the NaCl-brine is attributed to the formation of HCl from the hydrolysis of $MgCl_2$, as already discussed in session 2.3.

4. Stess corrosion cracking studies on carbon steels (ENRESA / INASMET)

The resistance of three preselected carbon steels to stress corrosion cracking is being examined in the $MgCl_2$-rich brine 1 (Q-brine, composition see Table I) by means of the slow strain rate technique (SSRT). The steels to be investigated are: the low-alloyed steels TStE 460 and 15MnNi6.3 (composition see Session 2.1) and the unalloyed fine-grained steel TStE 355 having the following composition in wt.%: 0.16 C; 0.41 Si; 1.5 Mn; 0.019 P + S; 0.036 Al; bal. Fe.

The experiments are being performed in Hastelloy C-276 autoclaves at strain rates of 10^{-4} - 10^{-7} s^{-1}, Temperatures of 25°C, 90°C and 170°C, and an argon pressure of 13MPa. In order to be able to interpret the results obtained in the brine, additional comparative investigations are being carried out in argon as an inert medium. Besides specimens made of the parent materials, also MAG (Metal Active Gas)

welded specimens simulating a possible packaging closure technique are being tested. Submerged-arc welded (SAW) specimens will not be examined because the results obtained so far (see section 2.3) have shown that this welding technique significantly reduces the corrosion resistance of the steels in $MgCl_2$-rich brines.

In the reporting time, stress corrosion cracking studies were perfomed on the parent materials in the brine and in argon at 170°C and strain rates of 10^{-4} s^{-1}, 10^{-5} s^{-1} and 10^{-6} s^{-1}.

4.1 Materials and experimental

The parent materials for TStE 355 (fine-grained steel) and TStE 460 were hot-rolled and annealed plates (2000 mm x 1000 mm x 15 mm), and for 15 MnNi 6.3 forged and annealed disks (30 mm thick). The mechanical properties of these steels are given in Table IV. The microstructures of the steels are shown in Fig. 9. For the TStE 355 and TStE 460 steels a ferritic microstructure with perlite bands typical of the rolling process was observed. A grain size value of 10 according to ASTM E-112 was measured for both steels. For the 15 MnNi 6.3 forged steel, a ferrite-perlite microstructure of a duplex grain size with an average value of 9 according to ASTM E-112 was observed.

For the MAG-welding of the specimens filler materials (Griduct SV-8 for TSt E 355, Thyssen Union K-5 Ni for TSt E 460 and 15 MnNi 6.3) were used. To characterize the weldments, metallographic studies were carried out.

For the slow strain rate tests, round specimens of 6 mm diameter were machined and finished with 1000 grade emery paper. The TSt E 355 and TSt E 460 specimens were machined in the transverse sense to the rolling direction of the plates, those of 15 MnNi 6.3 in the radial direction of the forged disks. The specimens were located in the Hastelloy C 276 autoclaves and attached to a fixed frame by one end and to the pull rod by the other. Fitting made of ZrO_2 ensured the electrical isolation of the specimens. Then the autoclave was filled either with Q-brine or argon, closed, pressurized and heated. Once the testing temperature and pressure were reached, the specimens were pulled until its fracture at the selected actuator displacement speed. A general view of the test equipment is shown in Fig.10.

Load, position, time and temperature data were continuously logged by the microprocessor that controls the testing machine. After each test, the elongation (E), reduction of area (R.A.), energy, yield strength (Y.S.) maximum load, and true stress at fracture were calculated. To examine whether secondary cracks were present, the fractured specimens were examined by metallography. Fractographic studies by means of scanning electron microscopy (SEM) are in progress.

4.2 Results

The results of the slow strain rate tests obtained so far for the three steels in argon and Q-brine at 170°C and various strain rates are given in Figs.11 and 12. The values are average of at least two tests. Compared to the values in argon, a clear diminishing of the elongation, reduction of area, energy and true stress at fracture occurred for all steels in Q-brine, mainly at strain rates of 10^{-5} s^{-1} and 10^{-6} s^{-1}. The values for the yield strength and maximum load in Q-brine, however, are very closed to those obtained in argon.

In the optical and metallographic examinations of specimens made of the hot-rolled steels TStE 355 and TStE 460, a non-uniform general corrosion due to local and repetitive breaking of the corrosion surface layer near the fracture zone was observed. Secondary cracks typical for stress corrosion cracking were not observed. For this reason, the reduction in ductility of these steels in Q-brine cannot be attributed to stress corrosion cracking. For the loss of ductility in this brine other mechanisms such as strengthening or embrittlement could be responsible.

In case of the forged steel 15 MnNi 6.3, a clear susceptibility to stress corrosion cracking in Q-brine was observed. In the metallographic examinations, besides a non-uniform general corrosion, extensive lateral secondary cracks were identified after testing in this brine at a strain rate of 10^{-5} s^{-1} (Fig. 13).

To examine the fracture surface morphology of the steels, fractographic studies by means of a scanning electron microscope are in progress. Furthermore, stress corrosion cracking studies in argon and Q-brine at 25°C and 90°C are under way.

5. Conclusions

In salt brines relevant for a rock-salt repository the low-alloyed steels TStE 460 and 15 MnNi 6.3 are subjected to non-uniform general corrosion. The corrosion rates obtained after a testing time of up to 1 year in the brines at 150°C (29 - 72µm/a in NaCl -brine, 90-175µm/a in $MgCl_2$-rich brines) imply corrosion allowances technically acceptable for thick-walled packagings with a service life of about 300 years, as discussed here. Pitting corrosion was not observed for the parent materials. Submerged arc welding (SAW) do not influence the corrosion behaviour of the steels in NaCl-rich brine. In $MgCl_2$-rich brines, however, severe local corrosion attacks in the heat-affected zone of the SAW-specimens occurred for both steels.

According to the results obtained so far from slow strain rate tests, the hot -rolled steels TStE 460 and TStE 355 (unalloyed fine-grained steel) are resistant to stress corrosion cracking in $MgCl_2$-rich brines at 170°C and strain rates of 10^{-4} -10^{-6} s^{-1}. On the contrary, the forged steel 15 MnNi 6.3 showed a high susceptibity to stress corrosion cracking under these conditions.

The in-situ corrosion results confirmed that the passively corroding alloy Ti 99.8-Pd is a promising corrosion protection material for carbon steel packagings in case of an attack of salt brines. On the basis of the results available from laboratory-scale and in-situ investigations, neither pitting and crevice corrosion nor stress corrosion cracking are expected, and the general corrosion is negligible (< 1µm/a). Carbon steel containers plated with Hastelloy C4 can ensure a long-term corrosion protection of the HLW forms in case of an attack of NaCl-brines. By attack of $MgCl_2$-rich brines, however, long-term barrier function cannot be expected from such containers because of the susceptibility of Hastelloy C4 to local corrosion.

Further corrosion studies on carbon steels, Ti 99.8-Pd and Hastelloy C4 are in progress. They focus above all on the clarification of the role of high temperature (150°C) during corrosion under gamma irradiation and on the performance of further stress corrosion cracking and in-situ experiments.

6. References

[1] E. Smailos, "Korrosionsuntersuchungen an ausgewählten Werkstoffen als Behältermaterial für die Endlagerung von hochradioaktiven Abfallprodukten in Steinsalzformationen", KfK 3953 (1985).

[2] E. Smailos, W. Schwarzkopf, R. Köster et al., "Corrosion Testing of Selected Packaging Materials for Disposal of High-Level Waste Glass in Rock Salt Formations", KfK 4723 (1990).

[3] R.E. Westerman, J.H. Haberman et al.; " Corrosion and environmental-mechanical characterization of iron-base nuclear waste package structural barrier materials", PNL Report No. 5426 (1986).

[4] W. Schwarzkopf, E. Smailos, R. Köster, "Langzeitbeständige Korrosionsschutzumhüllung für dicht verschlossene Gebinde mit hochradioaktivem Inhalt", DE-OS 34 47 278 (June 1986).

[5] W. Schwarzkopf, R. Köster, "Längszylindrischer Behälter für die Endlagerung von einer oder mehreren mit hochradioaktiven Abfällen gefüllten Kokillen", DE-OS 36 10 862 (Oktober 1987)

[6] W. Schwarzkopf, E. Smailos, R. Köster, "In-Situ Corrosion Studies on Cast Steel for a High-Level Waste Packaging in a Rock-Salt Repository", Mat. Res. Symp., Proc. Vol. 127, pp. 411-418, Materials Research Society (1988).

[7] E. Smailos, W. Schwarzkopf, R. Köster, "Corrosion behaviour of container materials for the disposal of high-level wastes in rock salt formations", Nuclear Science and Technology, CEC - Report EUR 10400 (1986).

[8] G.P. Marsh, G. Pinard-Legry, E. Smailos et. al., "HLW Container Corrosion and Design", Proc. of the Second European Community Conference on Radioactive Waste Management and Disposal, Luxembourg, April 22-26, 1985, p. 314.

[9] R.E. Schmitt, R. Köster, "Elektrochemische Korrosionsuntersuchungen an metallischen Verpackungsmaterialien für hochaktive Abfälle. Verhalten von Hastelloy C4 in quinärer Salzlösung und 1M NaCl", KfK Report No. 4039 (1986).

[10] E. Smailos, R. Köster," Corrosion Studies on Selected Packaging Materials for Disposal of High-Level Wastes", Proc. of a Technical Committee-Meeting of the IAEA on Materials Reliability in the Back End of the Nuclear Fuel Cycle, Vienna, September 2-5, 1986, IAEA-Tecdoc - 421, p. 7.

Table I: Compositions, pH -values and O_2 -contents of the salt brines used in the laboratory - scale corrosion experiments

Brine	Composition (wt.%)							
	NaCl	KCl	$MgCl_2$	$MgSO_4$	$CaCl_2$	$CaSO_4$	K_2SO_4	H_2O
1	1.4	4.7	26.8	1.4	---	---	---	65.7
2	0.31	0.11	33.03	---	2.25	0.005	---	64.3
3	25.9	---	---	0.16	---	0.21	0.23	73.5

pH (25°C): 4.6 for brine 1; 4.1 for brine 2; 6.5 for brine 3
O_2(55°C): 0.8 mg/l for brine 1; 0.6 mg/l for brine 2; 1.2mg/l for brine 3

Table II: Linear corrosion rates of the unwelded steels TST E 460 and 15 MnNi 6.3 in the test brines at 150°C

Material	Corrosion rate (µm/a)		
	Brine 1	Brine 2	Brine 3
TStE 460	175.2	90.0	29.0
15 MnNi 6.3	127.5	112.0	72.0

brines 1 and 2: $MgCl_2$ - rich; brine 3: NaCl - rich
test duration: 4 - 12 months

Table III: Maximum penetration depth of corrosion in the HAZ[+)] of the submerged arc welded steels TStE460 and 15 MnNi 6.3 after 12 months exposure to brines at 150°C

Material	Maximum penetration depth (mm)		
	Brine 1	Brine 2	Brine 3
TStE 460	1.5	2.2	0.05
15 MnNi 6.3	1.8	3.9	0.08

[+)] heat - affected zone

Table IV: Mechanical properties of the parent materials investigated in the slow strain rate tests

Steel		Y.S. (0.2%) (MPa)	U.T.S. (MPa)	E (%)	R.A.(%)
TSt E 355	T	419	566	27	61
	L	427	568	28	64
TSt E 460	T	505	633	24	51
	L	510	635	26	53
15 MnNi 6.3	R	343	545	33	78
	Tg	340	484	29	78

T: Transversal; L: Longitudinal; R: Radial; Tg: Tangential; Y.S.: Yield Strength; U.T.S. = Ultimate tensile strength; E. Elongation; R.A.: Reduction of area

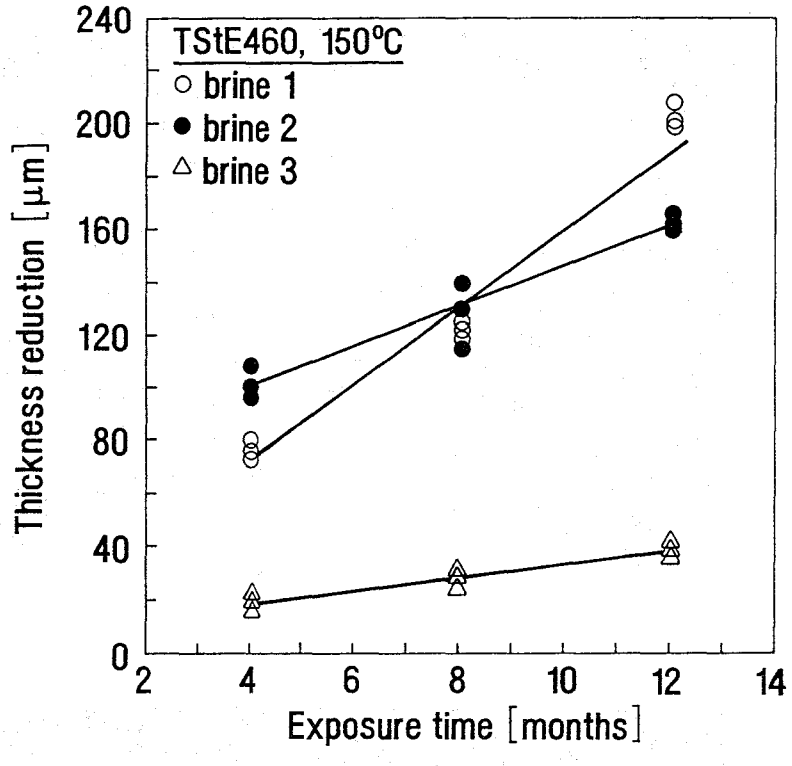

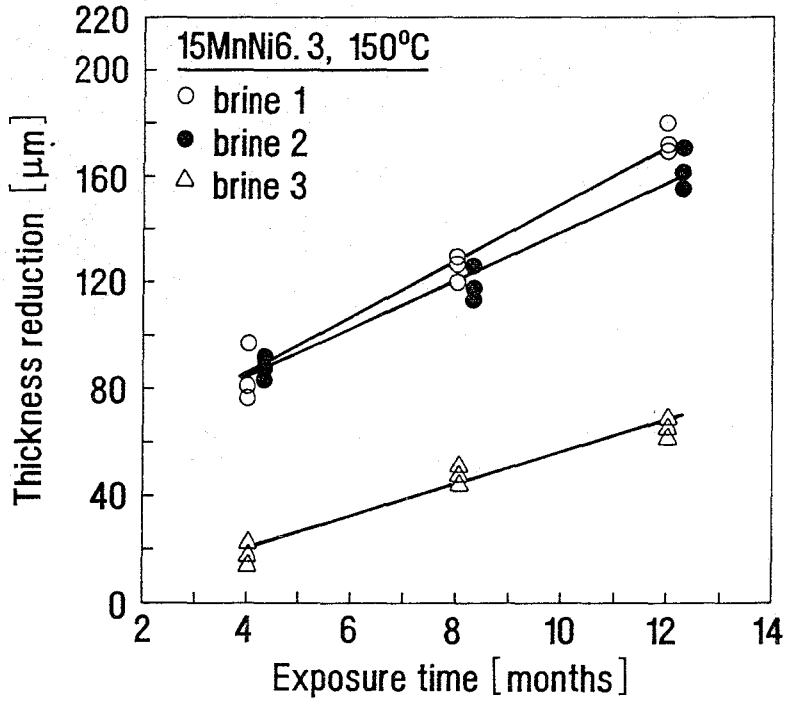

Fig. 1: Thickness reduction of the steels TSt E 460 and 15 MnNi 6.3 in salt brines at 150°C

TSt E 460

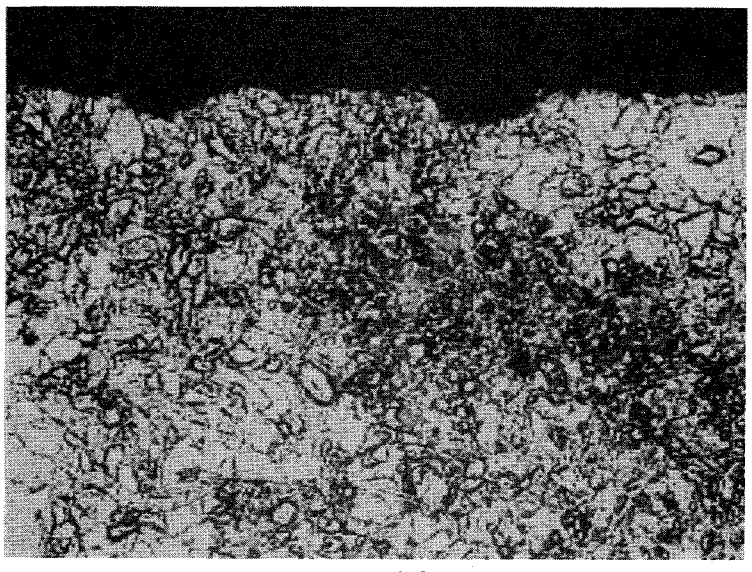

15 MnNi 6.3

Fig. 2: Optical micrographs of the unwelded steels TSt E 460 and 15 MnNi 6.3 after a 12-month exposure to brine 1(Q-brine) at 150°C (X 100)

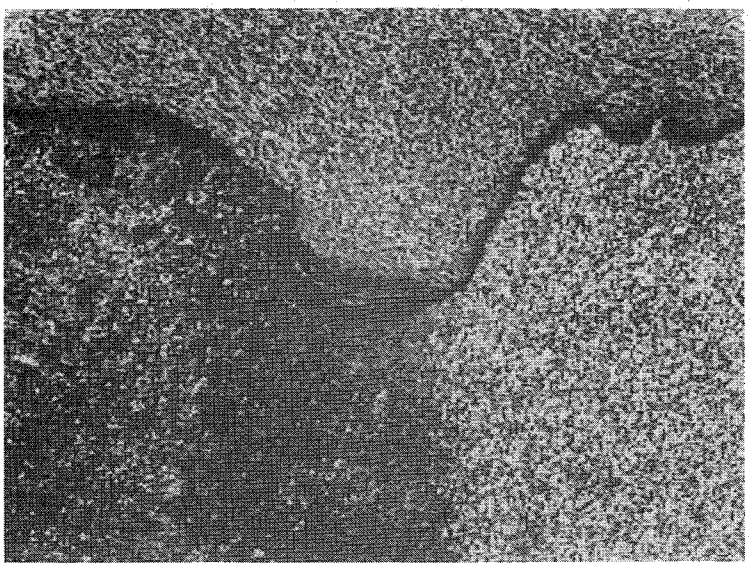

TSt E 460

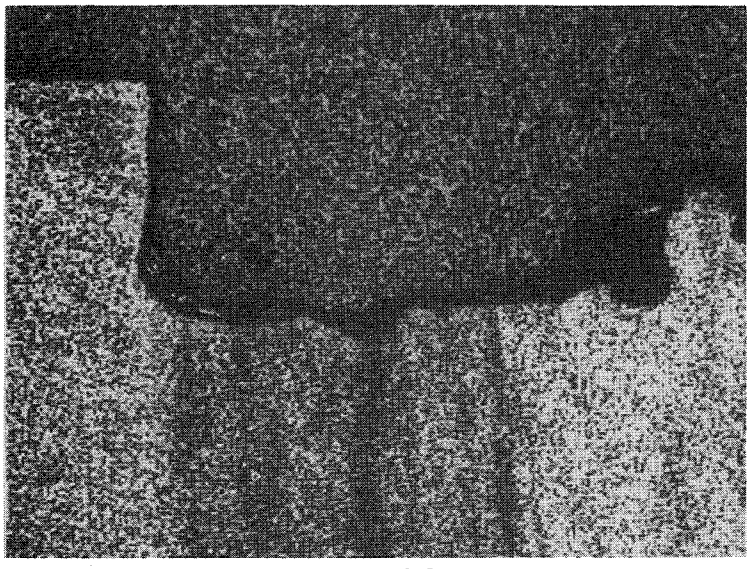

15 MnNi 6.3

Fig. 3: Optical micrographs of the submerged arc welded steels TSt E 460 and 15 MnNi 6.3 after a 12-month exposure to brine 1 (Q-brine) at 150°C (X 20)

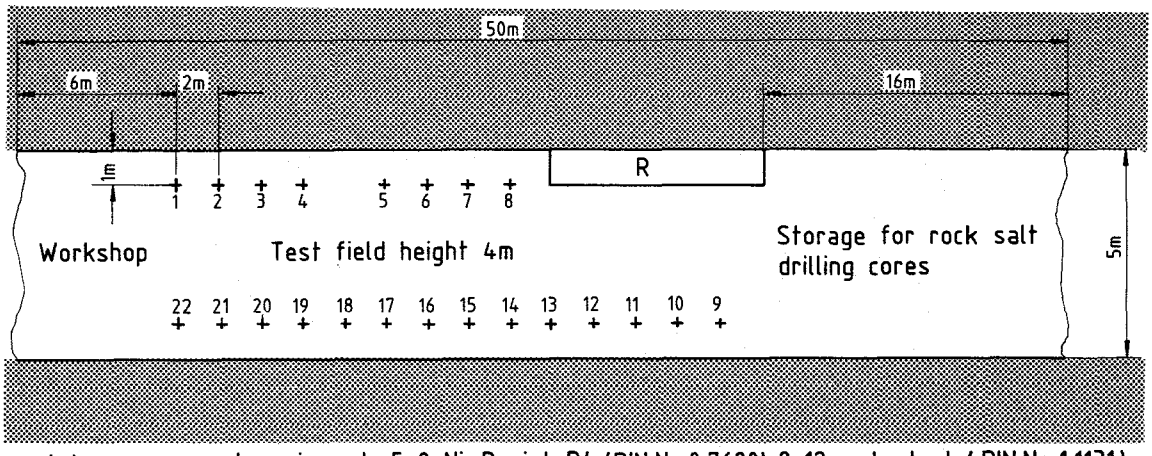

1-4 measurement equipment, 5-8 Ni-Resist D4 (DIN No.0.7680), 9-12 cast steel (DIN No.1.1131) 13-16 Ti 99.8-Pd (DIN No. 3.7025.10), 17-20 Hastelloy C4 (DIN No. 2.4610), 21-22 steel (DIN No.1.0841)
R reference experiments (metal sheets in rock salt at rock temperature)

Fig. 4: Layout of the in-situ corrosion test field on the 775 m level in the Asse salt mine and arrangement of the emplacement boreholes

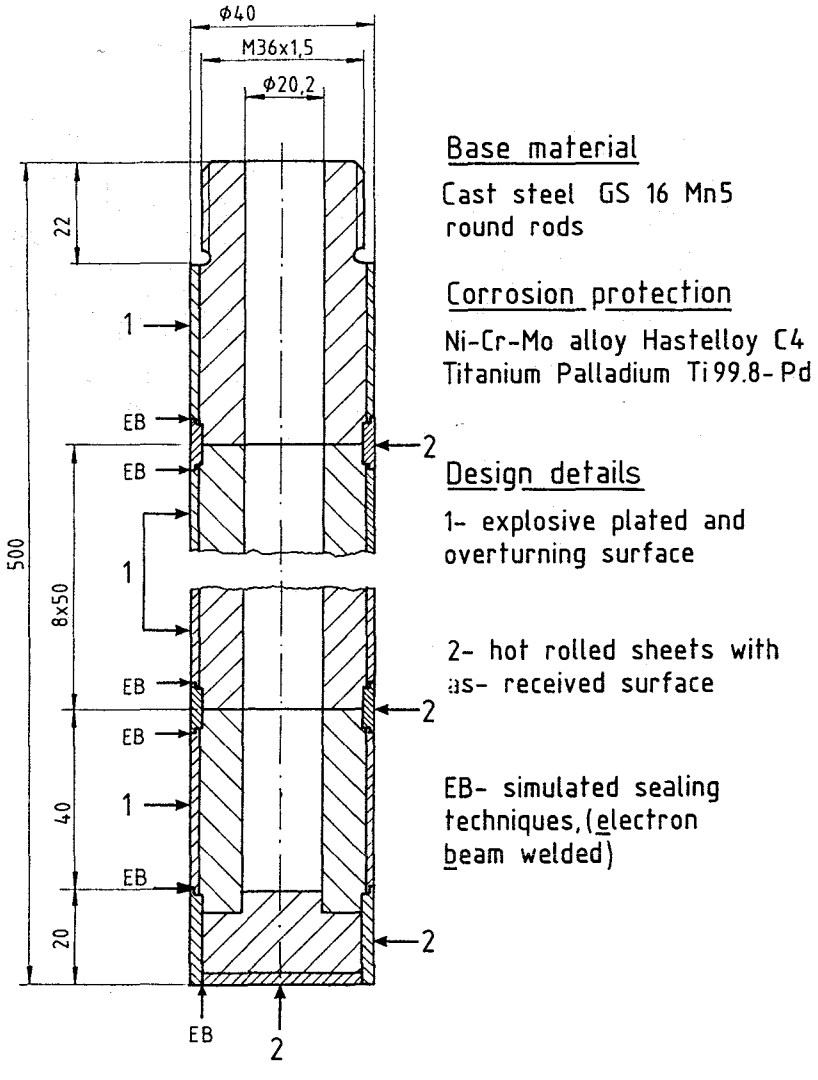

Fig. 5: Materials, dimensions, and manufacturing details of tubes investigated

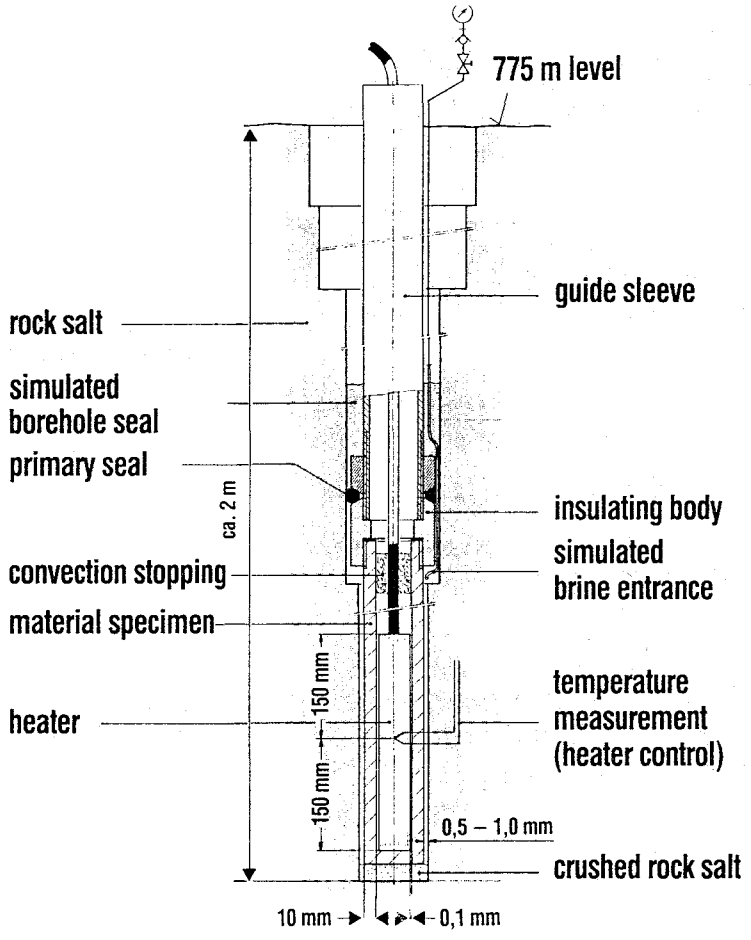

Fig.6: Vertical cross-section of the test assembly

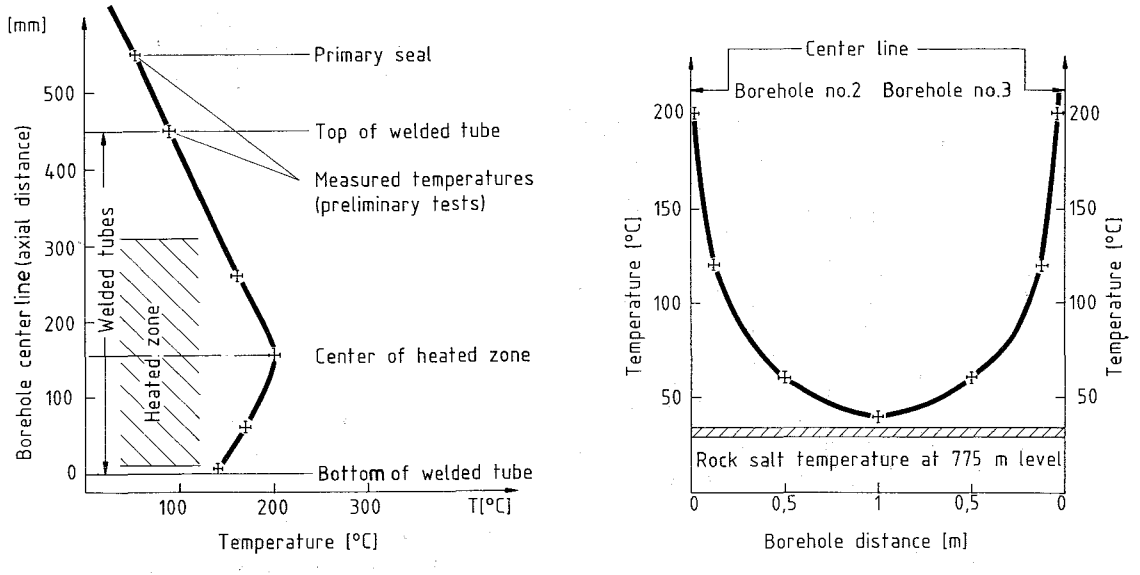

a) at the wall of the tubes

b) between two boreholes in the center of the heated zone

Fig.7: Temperature distribution at and between the test assembly

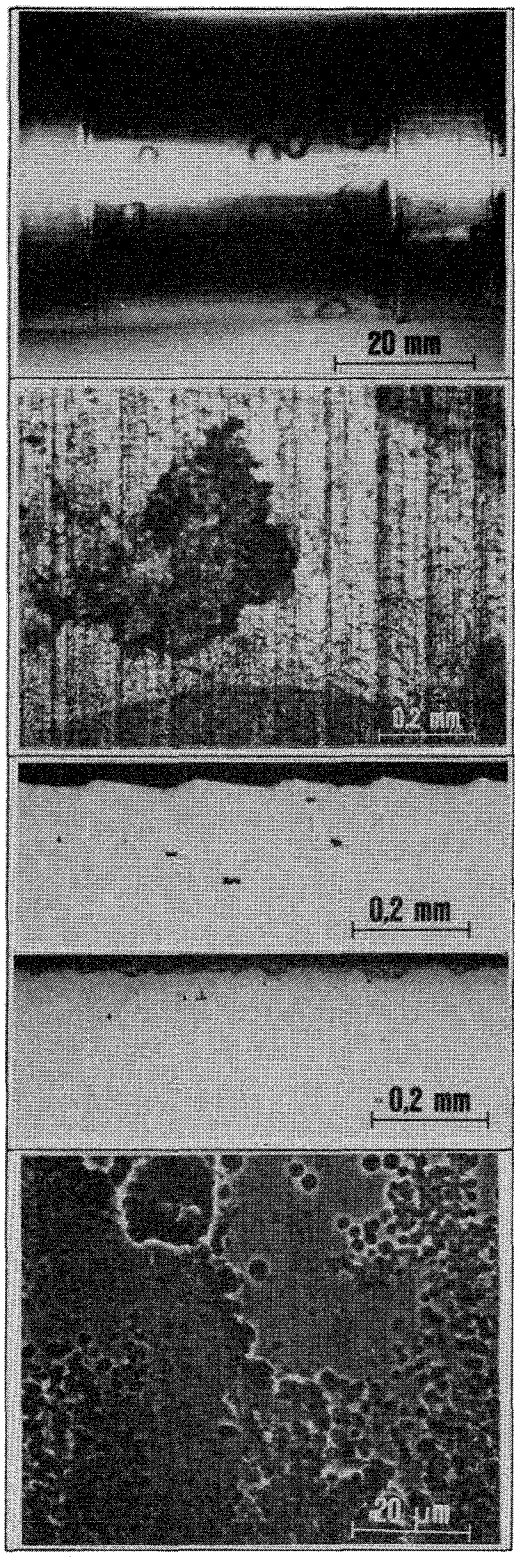

a) Optical macrograph of the surface of the tube section

b) Optical micrograph of the surface layer

c) Optical micrographs before exposure (above) and after exposure (below)

d) SEM photograph, detail of the surface layer

Fig.8: Corrosion of a cast-steel tube plated with Hastelloy C4 after in-situ storage (1.5 a in rock-salt + 100 ml added $MgCl_2$-rich Q-brine at 90°C-200°C)

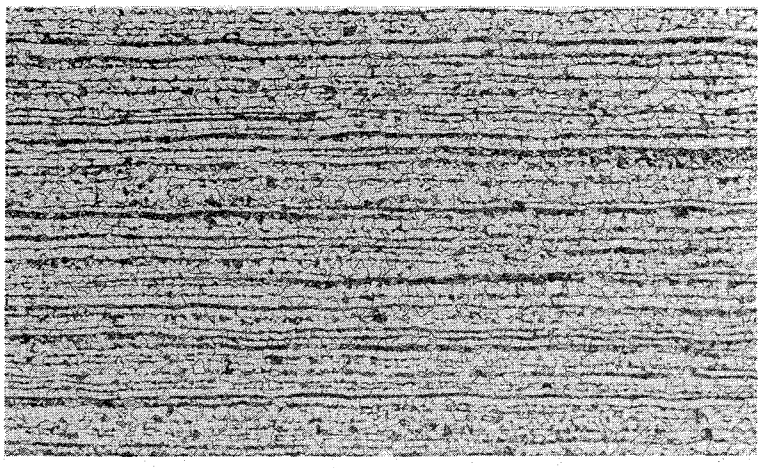

TSt E 355

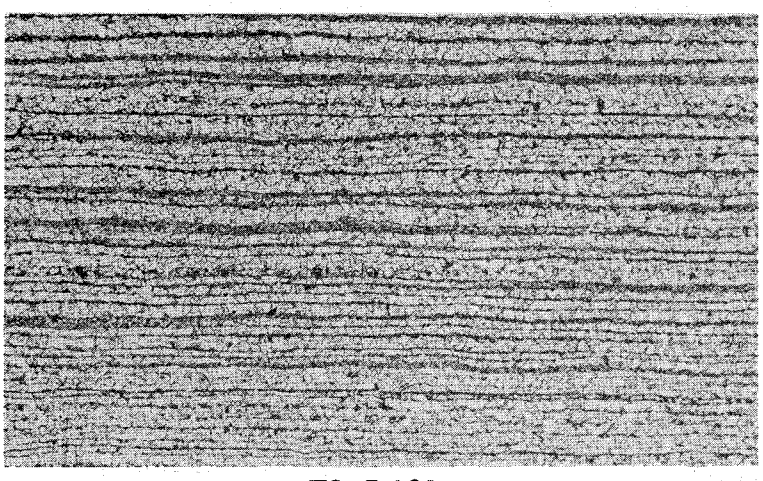

TSt E 460

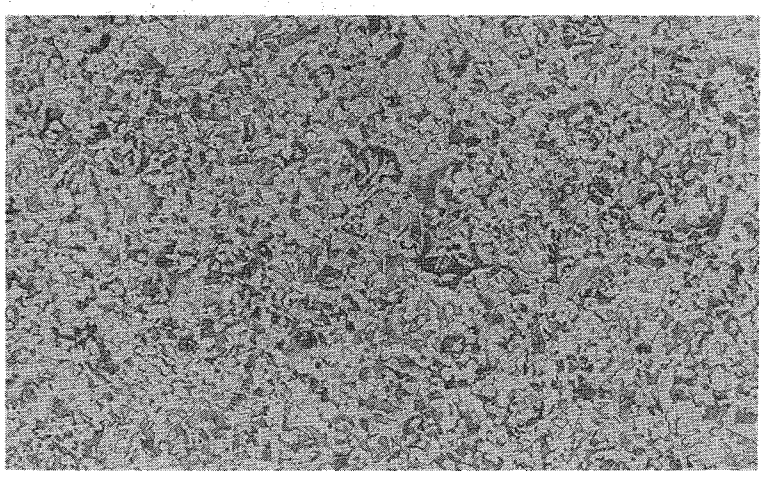

15 MnNi 6.3

Fig.9: Optical micrographs of the steels TSt E 355, TSt E 460 and 15 MnNi 6.3 used in the slow strain rate tests (X 100)

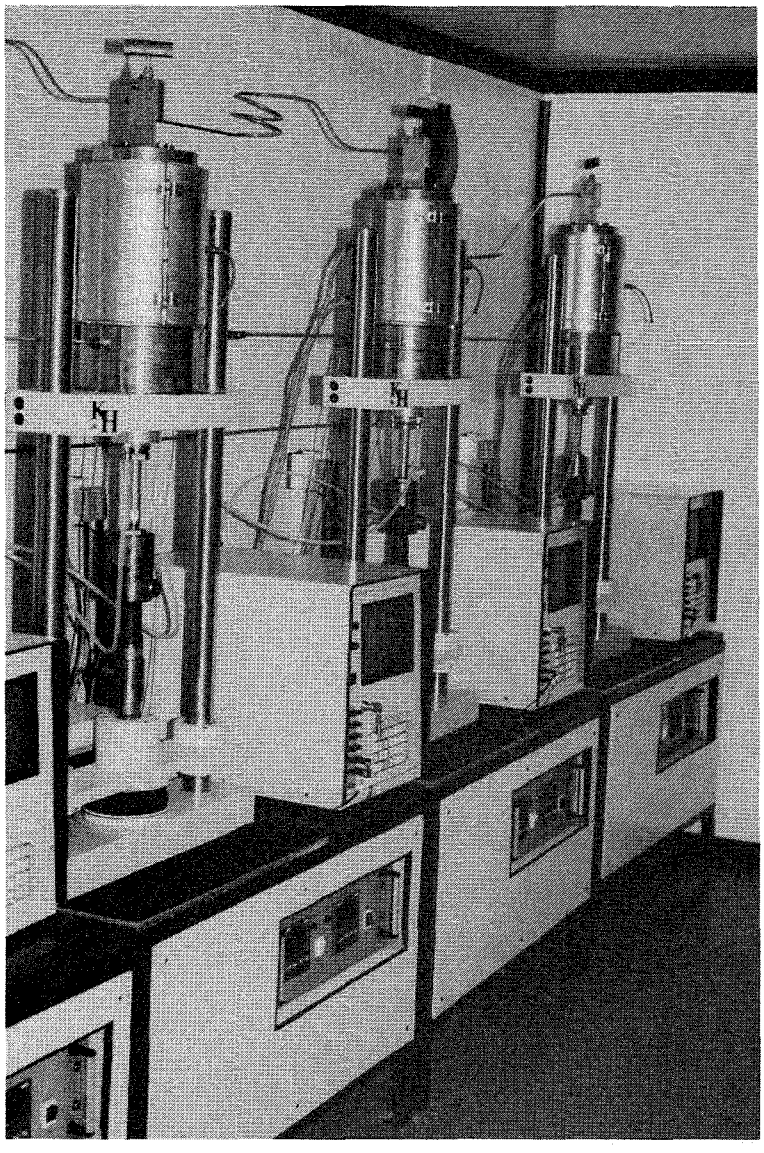

Fig. 10: Slow strain rate testing machine with autoclave

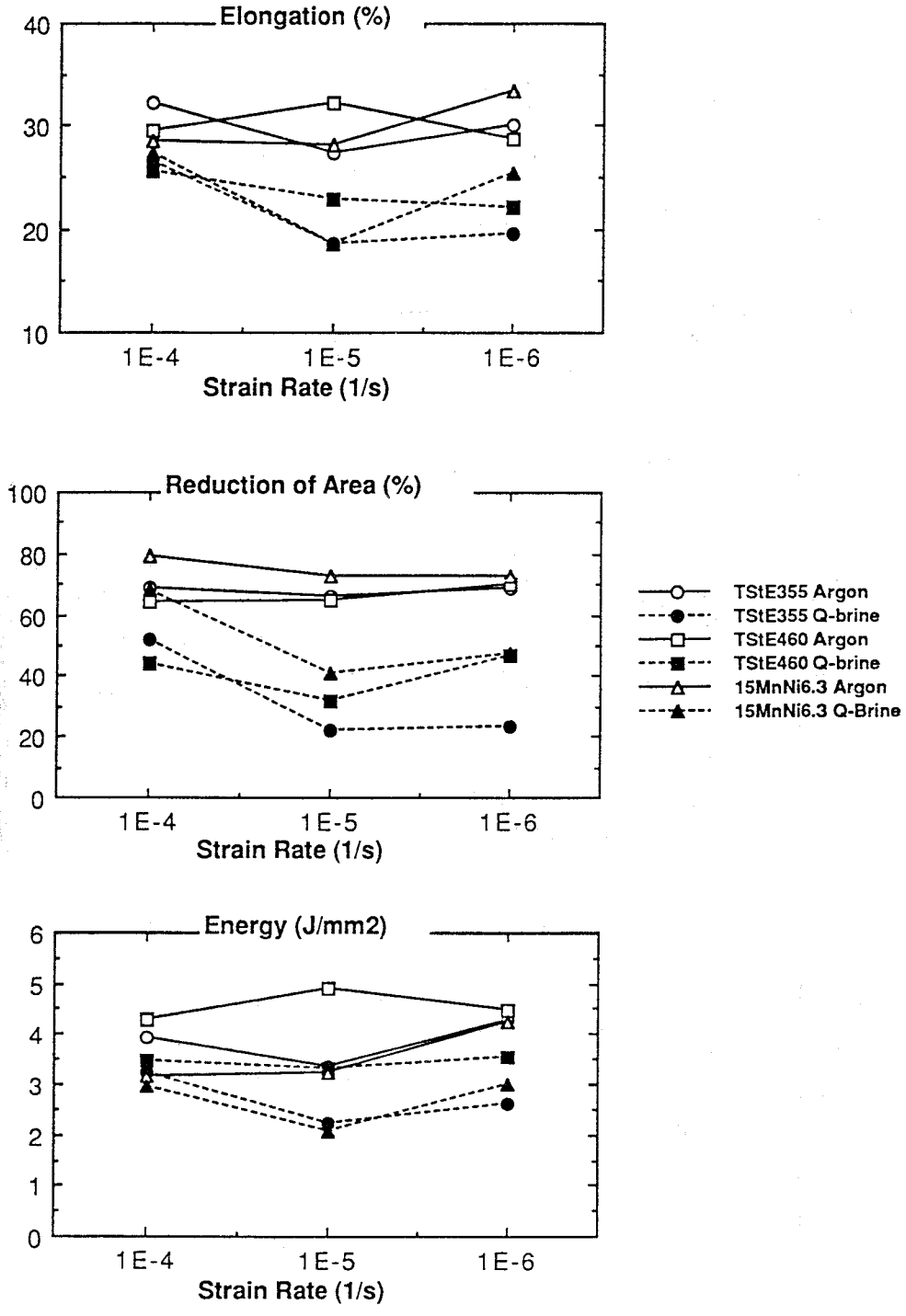

Fig.11: Elongation, reduction of area and energy versus strain rate for the TSt E 355, TSt E 460 and 15 MnNi 6.3 steels tested at 170°C and 13 MPa in argon and Q-brine.

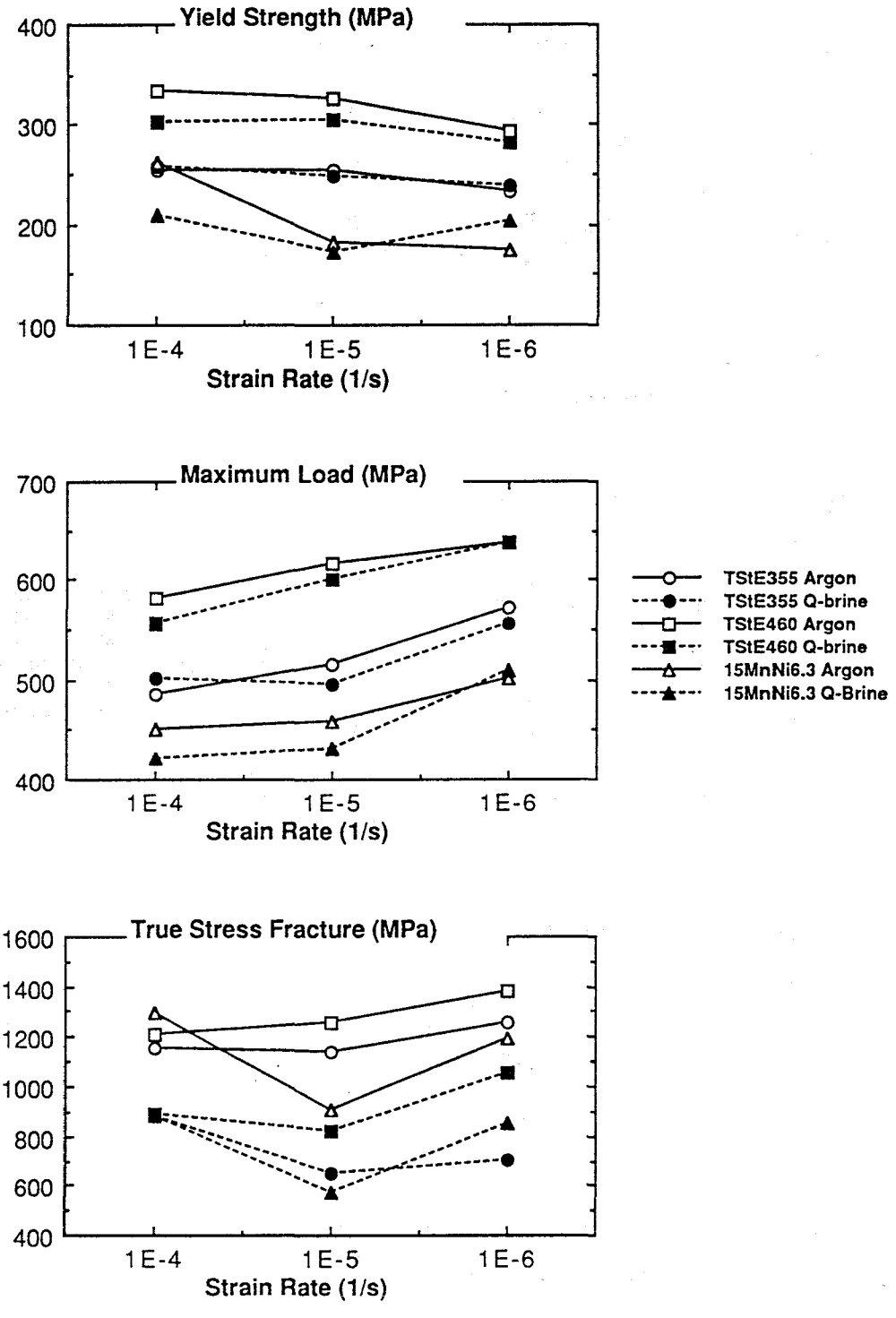

Fig.12: Yield strength, maximum load and true stress fracture versus strain rate for the TSt E 355, TSt E 460 and 15 MnNi 6.3 steels tested at 170°C and 13 MPa in argon and Q-brine

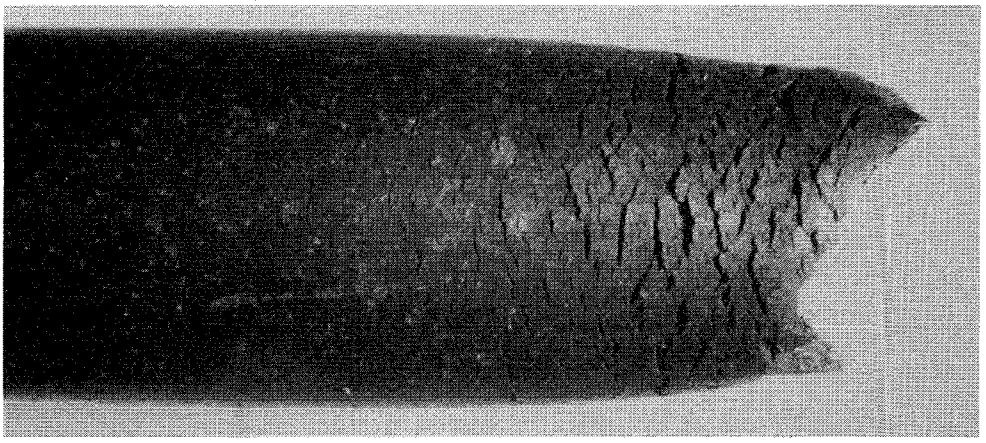

Fig.13: Extensive secondary cracking of the 15 MnNi 6.3 steel testedin Q-brine at 170°C, 13 MPa and 10^{-5} s^{-1}